Pathway of ADP-Stimulated ADP Release and Dissociation of Tethered Kinesin from Microtubules. Implications for the Extent of Processivity†

David D. Hackney*

Department of Biological Sciences, Carnegie Mellon University, 4400 Fifth Avenue, Pittsburgh, Pennsylvania 15213

Received November 8, 2001; Revised Manuscript Received January 31, 2002

ABSTRACT: Kinesin binds to microtubules with half-site ADP release to form a tethered intermediate with one attached head without nucleotide and one tethered head that retains its bound ADP. For DKH405 containing amino acid residues 1−405 of *Drosophila* kinesin, release of the remaining ADP from the tethered head is slow (0.05 s^{-1}), but release is accelerated by added ADP or ATP. The maximum rate of ADP-stimulated dissociation of tethered DKH405 from the microtubule is ∼12 s^{-1} as determined by turbidity. Parallel measurements of ADP-stimulated release of 2′(3′)-*O*-(*N*-methylanthraniloyl)-ADP (mantADP) from the tethered intermediate by fluorescence indicate that the reaction is biphasic with a fast phase that occurs at a rate that is similar to dissociation. The rate of the slow phase is dependent on the concentrations of salt and microtubules and is equal in each case to the rate for bimolecular stimulation of ADP release by microtubules as measured independently. These results are consistent with a scheme in which the fast phase, with approximately one-third of the total amplitude change, is due to ADP-stimulated release of mantADP from the tethered intermediate at ∼6 s^{-1}. This direct release of mantADP continues until terminated by dissociation of DKH405 from the microtubule at ∼12 s^{-1}. The majority of the amplitude change thus occurs through bimolecular recombination of DKH405·mantADP with microtubules following initial dissociation. Analysis of a simple scheme indicates that hydrolysis of ATP at the attached head before the tethered head can release its ADP and become tightly bound may be the principal limitation to processivity.

Kinesin is a motor protein that is responsible for transporting a range of membrane vesicles along MTs[1] (see ref *1* for review). An intriguing feature of the motility of kinesin is that it is processive with a single kinesin dimer being able to move for long distances along a MT without dissociation (*2*, *3*). The solution ATPase properties of short dimers of motor domains are in agreement with the requirements of a processive motor with a stoichiometry of 1 ATP per step of 8 nm (see ref *4* for discussion). The average number of ATP molecules hydrolyzed during each productive encounter of a dimeric motor with the MTs is ∼100 per dimer (*4*, *5*), which corresponds to an average sliding distance before dissociation of 800 nm at 8 nm per step and one step per ATP. Furthermore, the maximum ATPase rate at saturating levels of MTs is ∼80 s^{-1} per dimer, and this predicts a sliding velocity of 640 nm s^{-1} that is in good agreement with observed rates of single motor sliding (*6*). This conclusion has been supported by the measurement of both motility and ATPase with the same preparation (*7*).

In the absence of MTs the release of ADP is the rate-limiting step, but MTs stimulate net ATP hydrolysis by binding to the head·ADP complex and accelerating ADP release (*8*). When a dimer of motor domains binds to a MT in the absence of ATP, one head releases its ADP and becomes tightly bound to the MT whereas the other head retains its ADP and remains tethered to the MT by the attached head (*9*). The tethered head cannot release its ADP because the steric constraints in the dimer prevent it from being able to productively interact with the next tubulin binding site. The tethered intermediate (II in Schemes 1 and 2) is the predominant steady-state intermediate during steady-state MT-stimulated ATP hydrolysis at subsaturating ATP levels, and it accumulates to essentially stoichiometric levels (*9*). At saturating ATP, the turnover of the tethered intermediate is at least as fast as net hydrolysis (*10*−*12*). This tethered intermediate likely plays a central role in the processivity of kinesin as it provides a mechanism for the ATPase cycles of the two heads of the dimer to be out of phase and thus allows one head or the other to usually be tightly bound to the MT.

Although the general properties and significance of the tethered intermediate described above are now well established, important aspects of the steps leading into and out from the tethered intermediate are unknown or controversial (*10*−*12*), including the rate of release of the ADP from the tethered head, the extent of interaction of the tethered head with the MT, the nature of the rate-limiting step at saturating ATP, and the identity of the steps that limit processivity. This report presents a detailed analysis of the kinetics of reaction of the tethered intermediate of DKH405. It is shown that binding of ADP to the attached head both accelerates release of ADP from the tethered head and accelerates

† Supported by Grant NS28562 from the National Institutes of Health.

* To whom correspondence should be addressed. Tel: (412) 268-3244. Fax: (214) 268-7129. E-mail: ddh+@andrew.cmu.edu.

[1] Abbreviations: AMP-PNP, 5′-adenylyl imidodiphospahte; mantADP, 2′(3′)-*O*-(*N*-methylanthraniloyl)adenosine 5′-diphosphate; MT, microtubule.

10.1021/bi0159229 CCC: $22.00
Published on Web 03/06/2002

dissociation of the kinesin dimer from the MT. During processive ATP hydrolysis, the dissociation from the MT of species with ADP bound to the tethered head and ADP or ADP and P_i bound at the attached head may be the process that limits processivity.

MATERIALS AND METHODS

DKH405 was prepared as previously described (*5*). All concentrations for kinesin are given as the concentration of motor domains. The DKH405·mantADP complex was formed by dialysis of DKH405·ADP against solutions containing mantATP generally as described previously (*13*) except that the final dialysis was against A25 buffer (*14*) containing 20% glycerol, 50 mM KCl, 1 mM dithiothreitol, and 10 μM mantATP. Typically, the final concentration of the DKH405·mantADP complex was >200 μM, and bound mantADP was in large excess over the free mantADP at 10 μM. Tubulin was prepared and purified on phosphocellulose by the method of Williams and Lee (*15*). MTs were prepared by polymerization of tubulin in the presence of ≤50 μM GTP. Polymerization was initiated by warming to 35 °C and then completed by addition of Taxol in small aliquots to a total of 1.3 mol of Taxol per tubulin dimer. The MTs were then washed twice by centrifugation and resuspension at 25 °C in A25 buffer with 25 mM KCl and stored in small aliquots at −80 °C following fast freezing by immersion in liquid nitrogen. All solutions containing MTs were supplemented with Taxol to 10 μM. The tubulin concentration is expressed as the molar concentration of heterodimers of 110 kDa using an extension coefficient of 1.03 mL/(mg·cm) at 275 nm in 6 M guanidine hydrochloride. On the day of use, an aliquot of MTs was thawed at 25 °C and centrifuged for 1 min at 7500*g* to remove aggregates.

Fluorescence and Turbidity. Reactions were performed at 25 °C in A25 buffer supplemented with KCl as indicated. In all cases, ADP or ATP was added as the 1:1 magnesium complex. Stopped-flow fluorescence and turbidity experiments were performed on an Applied Photophysics SX.18 instrument. Excitation for fluorescence was at 356 nm, and emission was monitored through a 415 nm long-pass filter. Turbidity measurements were performed at 320 nm using the 10 mm path-length window of the stopped-flow cell. Measurements of fluorescence over longer time periods were performed by switching the fiber-optic lines (coming from the light source and going to the photomultiplier) from the stopped-flow observation cell to an open 4 mL fluorescence cell that was rapidly stirred by a magnetic stirring bar. The housing for the stirred cell contained a port that allowed rapid injection of small volumes of reagents without introduction of light. In most cases the data were oversampled at the maximum rate of the data acquisition system and then averaged to produce the reported data points. For the slow reactions in the stirred cell, the signal was also filtered with a time constant of 15 ms before digital acquisition. These signal processing methods, along with the large illuminated volume in the stirred cell, allowed fluorescence measurements to be performed at low concentrations of mantADP as in Figure 2A at 20 nM. The fast phase observed on addition of MgADP in Figures 5 and 6 could in part be due to contamination of the ADP stock with ATP. However, the stock of ADP that was used contained only 0.26% ATP as determined by assay with luciferase, and removal of this ATP by treatment with glucose and hexokinase did not produce any significant change in the rate or amplitude of the fast phase.

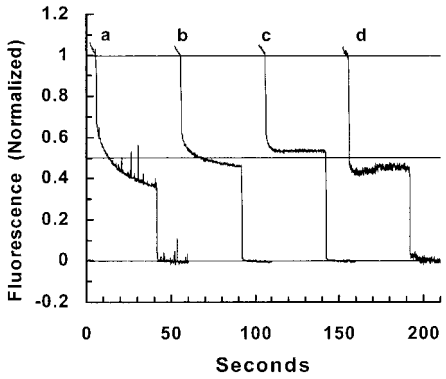

FIGURE 1: Dependence of mantADP release from the tethered head on the level of free mantADP. Each trace was initiated by addition of DKH405·mantADP, followed by addition of MTs to 1 μM after 6 s and MgATP to 200 μM after 42 s. Trace a was with 0.1 μM DKH405·mantADP, whereas traces b−d were with 0.25 μM DKH405·mantADP. Free mantADP was included before addition of DKH405·mantADP at 0.25 and 3 μM for traces c and d, respectively. Each trace was normalized to 1.0 for the value before addition of MTs and to 0 for the value after addition of ATP. Lines at normalized values of 0, 0.5, and 1 are included for illustration.

RESULTS

Characterization of the Steady-State Properties of the Tethered Intermediate. Previous reports have indicated a wide range of stabilities for the tethered intermediate (*9*, *10*, *12*), and Figure 1 presents characterization of the tethered intermediate for DKH405 in A25 buffer with 25 mM KCl. A general scheme for dissociation of mantADP in the presence of variable levels of ADP is given in Scheme 1. Addition of 1 μM MTs to 0.25 μM DKH405·mantADP in the absence of ATP (Figure 1, trace b) results in the rapid release of half of the mantADP on formation of II, with the other half being rapidly chased off by addition of excess ATP as observed previously with [^{32}P]ADP (*9*) and by fluorescence (*10*, *12*). The apparent amplitude of the first phase is only 0.4, but is close to 0.5 if corrected for the small increase in signal due to MTs alone. The subsequent slower loss of fluorescence is mainly due to partial net release of mantADP from the tethered head to form X and a much slower component due to equilibration of the 2′- and 3′-mantADP isomers (*13*). Inclusion of 0.25 or 3 μM free mantADP before addition of DKH405·mantADP (Figure 1c,d) suppresses this partial net release from the tethered head through rebinding of mantADP to X (rate constant k_{bi-D}) and produces a stable tethered intermediate. This is in agreement with the result of Ma and Taylor (*10*), who observed tight binding of mantADP to the tethered head. Conversely, reduction in the free mantADP concentration by lowering the initial DKH405·mantADP concentration to 0.1 μM (Figure 1a) results in more extensive net release of mantADP from the tethered head and accumulation of X. In Figure 2A, the DKH405·mantADP concentration has been further reduced to 0.02 μM, and the slow phase for release of mantADP from the tethered head is largely complete in the 36 s before addition of ATP. The theoretical line indicated in Figure 2A was calculated for release from the tethered head, k'_o, at 0.05 s^{-1} and a final amplitude of 0.1. This

Scheme 1: Scheme for Dissociation of mantADP in the Presence of ADP[a]

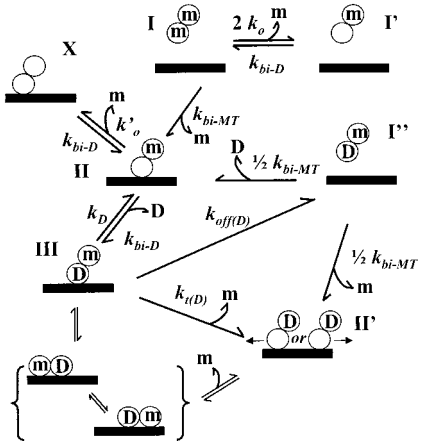

[a] The paired circles represent the DKH405 dimer, and the solid bar represents a MT. The (+) end of the MT is to the right. The scheme cannot indicate the many possible configurations of tethered intermediates such as II, III, and X. Drawing them with the tethered head detached from the MT and to the right is not intended to indicate that this is necessarily the predominant configuration, and some interaction of the tethered head with the MT is likely. ADP and mantADP are designated D and m, respectively. It is assumed that the rates with mantADP are the same as with ADP, and thus the rate for bimolecular stimulation of ADP release by MTs, k_{bi-MT}, is the same for release of mantADP and ADP. k_{bi-MT} is the bimolecular rate for binding of either a monomer or dimer motor construct to the MT with initial release of one ADP. The rate for conversion of I″ to II or II′ is only half of k_{bi-MT} because half of the events result in release of ADP and not mantADP. Note that a species with the same composition as III is transiently formed during conversion of I″ to II. $k_{bi-MT(T)}$ and $k_{bi-MT(D)}$ are the observed rates for bimolecular MT-stimulated ADP release in the presence of a chase by ATP or ADP, respectively. For a monomer, all three rates should be approximately equal. For a dimer, k_{bi-MT} and $k_{bi-MT(T)}$ should be equal because both ADP molecules are released on each productive encounter, but $k_{bi-MT(D)}$ may be up to 2-fold smaller as discussed in the text. Because no net input of energy occurs on going from II to II′ in the presence of ADP alone, no net directional movement can occur, and the new attachment position will shift one position toward the (+) or (−) ends of the MT with equal probability. The rate of nucleotide binding to kinesin is similar whether the head is bound to MTs or not, and the same rate constant, k_{bi-D}, is used in all cases. The rate of ADP release from kinesin, k_o, is measured as a probability per ADP. For a dimer like DKH405, the microscopic rate for conversion of I to I′ will be $2k_o$ because release can occur from either head.

process is likely to be complicated by some formation of the inactive conformation of nucleotide-free DKH405 (*14*), but the release rate of 0.05 s^{-1} is clearly significantly faster than the rate of 0.01 s^{-1} that is observed in the absence of MTs with DKH405 (*5*).

The dynamic nature of the tethered intermediate is indicated by the results of Figure 2B,C. For the trace in Figure 2B, a stable tethered intermediate was produced as in Figure 1c, and then at 18 s a small chase of ADP (2 μM) was added to trap released mantADP and prevent inactivation of the tethered head in the absence of nucleotide. The observed rate of 0.08 s^{-1} is still slow but is larger than the 0.05 s^{-1} value in Figure 2A due to the additional contribution from an ADP-dependent pathway (see Figure 3). Because there was only a 5-fold excess of ADP over mantADP, a significant amount of mantADP was still bound at the end of the transient and was released on addition of excess ATP. The initial part of Figure 2C is the same as in Figure 2B, but a substoichiometric pulse of ATP (0.1 μM) was added

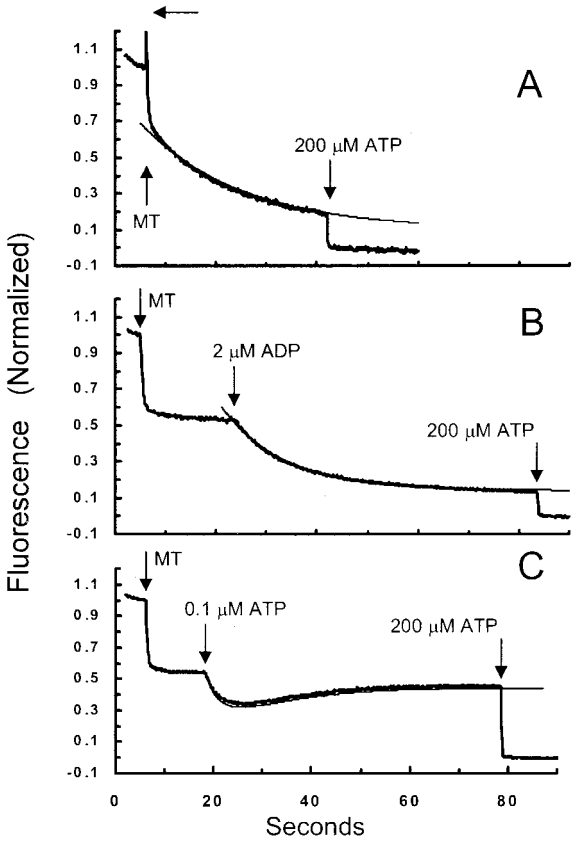

FIGURE 2: Kinetics of release of mantADP from the tethered head. Traces were normalized as in Figure 1 and are not corrected for the contribution of MTs alone. (A) Sequential addition of DKH405·mantADP (0.02 μM), MTs (0.4 μM), and MgATP (200 μM) at 0, 6, and 42 s, respectively. The thin line was calculated for a rate of 0.05 s^{-1} and a final normalized value of 0.1. (B) Sequential addition of DKH405·mantADP (0.25 μM), MTs (1 μM), ADP (2 μM), and MgATP (200 μM) at 0, 6, 24, and 84 s, respectively. The starting medium was supplemented with free mantADP at 0.25 μM, as in Figure 1c. The thin line was calculated for a rate of 0.08 s^{-1} and a final normalized value of 0.14. (C) DKH405·mantADP and MTs were added as in (B), but ATP was added to 0.1 μM and then 200 μM at 18 and 78 s, respectively. The thin line was calculated for the model of Scheme 2 starting with 0.25 μM tethered DKH405 with 0.125 μM mantADP bound to the tethered head and 0.375 μM free mantADP, using 2 μM^{-1} s^{-1} for the rate of ATP-induced release of mantADP or ADP from the tethered head and 0.06 s^{-1} for the average rate of exchange of the ADP or mantADP bound to the tethered head at ~0.5 μM total ADP and mantADP (see Figure 3).

at 18 s. Because binding of ATP to the attached head with subsequent release of mantADP from the tethered head is fast, there is an initial rapid drop in fluorescence as ATP binding to the attached head displaces bound mantADP from the tethered head to form a tethered intermediate with bound ADP and not mantADP. This transiently leaves the tethered head enriched in bound ADP while the larger pool of free nucleotide is mainly mantADP. Subsequent reversible release of ADP from the tethered head at ~0.06 s^{-1}, however, reestablishes the equilibrium and repopulates the tethered head with mantADP with recovery of most of the initial loss of fluorescence.

ADP-Stimulated Release of mantADP from the Tethered Intermediate. Stopped-flow experiments were used to determine the ADP dependence of the release of mantADP from the tethered intermediate as indicated in Figure 3. A stable tethered intermediate was generated in the presence

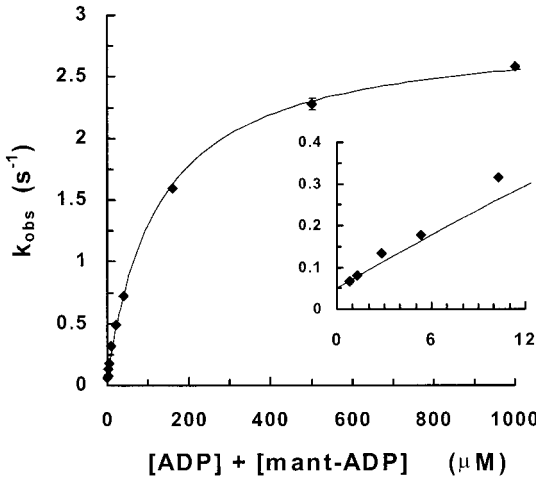

FIGURE 3: Dependence on ADP of the rate for mantADP release. A stable DKH405·mantADP·MT tethered intermediate was generated from 4 μM MTs, 0.8 μM DKH405·mantADP, and 0.2 μM mantADP (2× concentrations) and mixed 1:1 in the stopped flow with solutions containing MgADP. The indicated line was obtained by nonlinear regression using a fixed value of 0.05 s^{-1} for the intercept and varying the maximum rate and $K_{0.5}$ to obtain 2.82 s^{-1} and 126 μM, respectively.

of sufficient free mantADP to maintain saturation of the tethered head with mantADP, and this complex was then mixed with ADP. The value of 2.8 s^{-1} for the maximum rate under these conditions is consistent with previous reports (*10*, *12*). The low value of 0.05 s^{-1} for k'_o indicated by the intercept in the absence of ADP (Figure 3, insert) is in agreement with the results of Figures 1 and 2. Parallel experiments with DKH560 yielded a similar rate of 0.09 s^{-1} (not shown), and previous work with DKH392 (*9*) indicated a low value for k'_o. Ma and Taylor (*10*) have also reported a low rate for k'_o of 0.13 s^{-1} for human kinesin. Other work, however, has reported variable faster rates of 0.4−2.3 s^{-1} (*12*) for k'_o with a very similar construct of *Drosophila* kinesin, K401. The basis of this discrepancy is unclear. Even trace amounts of ATP that were carried over from previous experiments in the stopped flow would greatly accelerate the observed rate of loss of mantADP from the tethered head, and this could be a factor in some cases. An additional possible factor is the presence of GTP, which also accelerates release of mantADP from the tethered head (*10*). The MTs used in the present study were polymerized in the absence of added GTP and were washed twice by centrifugation and likely contain negligible levels of free GTP.

ADP-Induced Dissociation of the Tethered Intermediate. Light scattering and turbidity can be used to monitor the dissociation of motor domains from the MT; however, there is often a substantial flow artifact with MTs that limits the usefulness of these methods, and it is important to compare transient and steady-state measurements. Control experiments in a spectrophotometer using a stirred cuvette indicate that the A_{320} of 1.0 μM MTs in A25 buffer with 25 mM KCl is typically 0.045−0.05 and increases by 0.017 on binding of 0.6 μM DKH405. This relative increase in turbidity is approximately equal to the increase in mass per unit length along the MT (0.6 DKH405 motor domains per tubulin heterodimer). Addition of MgADP to 2 mM results in extensive dissociation in 50 or 100 mM KCl but only partial dissociation in 25 mM KCl. The results of Figure 4 indicate that similar absolute and relative changes are observed in

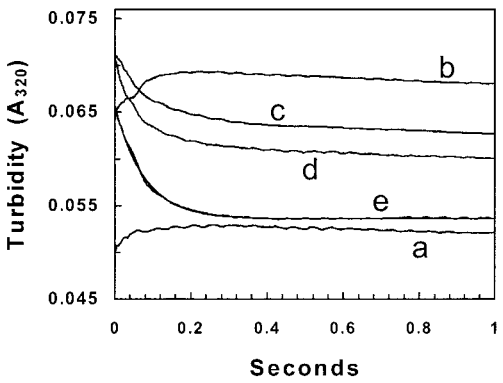

FIGURE 4: ADP-induced dissociation of MT·DKH405·mantADP. MTs at 2 μM (2×) in A25 with 25 mM KCl, with or without DKH405, were mixed 1:1 in the stopped flow with solutions containing variable levels of ADP and KCl as indicated, and the turbidity was monitored by measuring the absorbance at 320 nm using a 1 cm path length. For traces a−c, the other syringe contained A25 buffer with 75 mM KCl (2×) so that the final KCl concentration was 50 mM. For trace d, the other syringe contained 175 mM KCl for a final concentration of 100 mM. Trace a is for MTs alone. For traces b and c, the MT·DKH405·mantADP complex at a ratio of 0.6 head per tubulin dimer was preformed by combining 2 μM MTs with 1.2 μM DKH405·mantADP in A25 buffer containing 25 mM KCl before mixing in the stopped flow. At this concentration, the absorbance of the mantADP is negligible. For traces a and b the other syringe did not contain ADP, whereas for traces c and d, the other syringe contained MgADP for a final concentration of 2 mM (1×). Trace b was subtracted from trace c to give trace e. The offset of trace e was adjusted so that it had the same initial turbidity as trace b. The thin line is the best fit of trace e to a first-order reaction and has a rate of 13.2 s^{-1} and amplitude of 0.0122.

the stopped flow. Mixing MTs or the MT·DKH405 complex with buffer alone in the stopped flow (traces a and b) results in an increase in absorbance over the first 0.2 s that is followed by a slow decrease over the next 5 s. Similar flow artifacts are observed on mixing MTs with buffer containing ADP or with solutions of higher salt (not shown). When the MT·DKH405 complex is mixed with MgADP and KCl to final concentrations of 2 and 50 mM, respectively (trace c), the absorbance falls, indicating dissociation. The true net ADP-induced turbidity transient is given by trace e, which was obtained by subtracting trace b from trace c and adjusting the offset so that it has the same initial value as trace b for comparison. The difference in the initial values of traces b and c is mainly due to the presence in trace c of 2 mM ADP, which has an absorbance of ∼0.004 when measured under these conditions in the stopped flow. Trace e is the average of seven runs, which show considerable individual variation but are all approximately first order and have an average rate of 13.3 ± 0.6 s^{-1}. The amplitude of trace e is 0.0122, and the good agreement with the expected value of 0.014 from steady-state measurements indicates that the rate of 13 s^{-1} does represent the actual rate of dissociation, independent of the flow artifact. At a final KCl concentration of 100 mM (trace d) the corrected transient has an amplitude of 0.0138 and a rate of 15.3 s^{-1}. At a final KCl concentration of 25 mM, a smaller decrease in turbidity with a similar rate is observed when many traces are averaged, but the data are too variable to justify calculation of a rate constant. Ma and Taylor also reported a similar $k_{off(D)}$ value of 12 s^{-1} for a human kinesin dimer based on light scattering measurements (*16*).

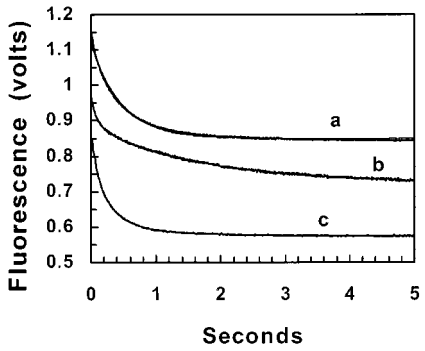

FIGURE 5: Salt and MT dependence of ADP-stimulated release of mantADP from the tethered intermediate. Stopped-flow conditions are as in Figure 4 except that fluorescence was monitored with excitation at 356 nm. One syringe contained 2 μM MTs and 1.2 μM DKH405·mantADP, and the other syringe contained 4 mM MgADP and variable KCl and MTs. Final KCl concentrations were 25 mM in trace a and 50 mM in traces b and c. For trace c, the second syringe contained 20 μM MTs for a final MT concentration of 11 μM after mixing. Offsets have been applied to the initial voltages for presentation on the same axis, but the amplitudes have not been adjusted.

Biphasic Release of mantADP at High Salt. Under the conditions of Figure 3 the transients for ADP-stimulated release of mantADP were approximately first order as indicated by trace a of Figure 5 , which is also in 25 mM KCl and has a rate constant of 2.5 s^{-1}. However, trace b of Figure 5 at 50 mM KCl is markedly biphasic. Trace b can be fit by a double exponential with rate constants of 9.9 and 0.6 s^{-1} and an amplitude of the fast component that is 33% of the total. At 100 mM KCl in Figure 6A, the curve is even more strongly biphasic with at similar fast rate but a greatly reduce rate for the slow phase of 0.078 s^{-1}. The fast phase in not well-defined in the insert to Figure 6A because of the wide spacing of the data points in this long analysis but is better defined at 16.5 s^{-1} in Figure 6B with acquisition over a 1 s range. Thus the turbidity transient and the fast phase of the fluorescence transient have similar rates, but the majority of the total amplitude (70%) for mantADP release occurs during a much slower phase at higher salt concentration. Alignment of the transients at different KCl concentrations (Figure 6B) indicates that all three plots have the same initial velocity, but at higher salt the velocity decreases rapidly. The rates for the slow phases (after 0.3 s) at 25, 50, and 100 mM KCl in Figures 5 and 6 are 2.03, 0.77, and 0.09 s^{-1}, respectively, when fitted by a single exponential with a slow linear term that is likely due to isomerization of the 2′- and 3′-mantADP isomers as discussed previously (*13*).

These results are consistent with a mechanism in which the true rate, $k_{t(D)}$, for ADP-induced release of mantADP from the tethered intermediate is ~6 s^{-1} and continues until terminated by dissociation of DKH405 from the MT at ~12 s^{-1} for $k_{off(D)}$. Further ADP release is limited by the rate of bimolecular recombination of DKH405 with the MT, which is very slow at high salt (*13*, *16*). As a test of this model, the apparent rate of bimolecular MT-stimulated mantADP release was determined in the presence of an ADP chase by mixing DKH405·mantADP in the stopped flow with MTs and ADP. In this reaction, the final concentrations of DKH405·mantADP, MTs, and ADP are the same as in Figures 5 and 6 with the only difference being the order of addition. The values that were obtained at 1 mM MgADP

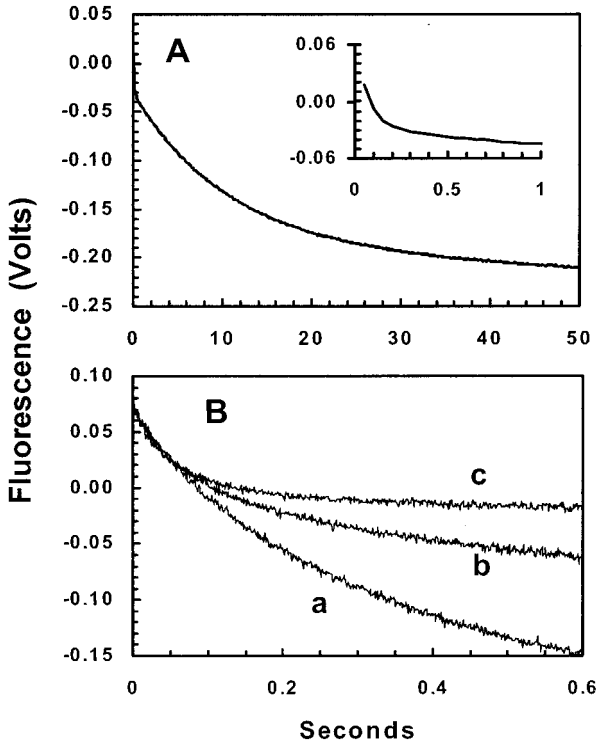

FIGURE 6: ADP-induced release of mantADP from the tethered intermediate at 100 mM KCl. (A) As in traces a and b of Figure 5 except at a final concentration of 100 mM KCl. (B) Overlay of transients at 25, 50, and 100 mM KCl (traces a−c respectively) for acquisition over a 1 s time period. The offsets have been adjusted slightly so that they have the same initial value for comparison. The amplitudes have not been adjusted and are directly comparable.

are 2.30 ± 0.01, 0.91 ± 0.02, and 0.118 ± 0.001 s^{-1} at 25, 50, and 100 mM KCl, respectively. These rates are essentially the same as the rates for the slow phase at each KCl concentration. The observed transient at 25 mM KCl (Figure 5, trace a) approximates a single first-order process because the rates of the fast and slow phases are similar at ~18 and ~2 s^{-1}, and this also likely accounts for the failure of previous studies to detect the underlying biphasic nature of the transients.

MT Dependence of ADP-Induced Release of mantADP from the Tethered Intermediate. Conversely, increasing the MT concentration at high salt will increase the net rate of bimolecular association of DKH405 with MTs and thus should accelerate the slow phase. Trace c of Figure 5 was performed identically to that of trace b, except that the syringe with the ADP also contained 20 μM MTs for a final concentration of 11 μM after mixing. At this higher MT level the slow phase is greatly accelerated and the transient is approximately first order at 4 s^{-1}. Note that the extra MTs accelerate the rate of mantADP release from the tethered intermediate even when added from the other syringe in trans. Thus the extra MTs exert their effect bimolecularly following dissociation of DKH405 from the original tethered complex. Parallel experiments with the extra MTs added in cis (22 μM MTs and 1.2 μM DKH405·mantADP in one syringe and only ADP in the other syringe) result in an approximately first-order transient of similar rate constant (not shown). This result indicates that lattice crowding effects are not likely to be significant as the same rates are seen in the cis case where the starting head:tubulin ratio is low. Extra MTs in trans also accelerate the apparent rate at 25 mM KCl to 5.1 s^{-1}. In

100 mM KCl, the transient is still biphasic with extra MTs in trans, but the rate for the slow phase is now 1.24 s^{-1} when evaluated from 0.3 to 5 s with a linear component. This rate is in agreement with the rate expected on the basis of the $k_{bi-MT(D)}$ value (11 μM MTs × 0.118 μM^{-1} s^{-1} = 1.3 s^{-1}).

ATP versus ADP Chase for Bimolecular Stimulation of mantADP Release by MTs. Rapid ADP-induced dissociation from the MT suggests that bimolecular release of mantADP from the combination of MTs with free DKH405·mantADP is largely a double-pass process for an ADP chase in which release of both mantADP molecules per dimer usually requires two or more productive diffusional encounters of DKH405 with a MT. If the tethered complex has $k_{t(D)}$ and $k_{off(D)}$ values of 6 and 12 s^{-1}, respectively, then an extra 0.33 ADP molecule will be released on average from the tethered head before dissociation of the dimer from the MT, and an average of 1.67 encounters will be needed for complete mantADP release. In contrast, mantADP release is expected to be a single-pass process when ATP is used as the chase nucleotide because both mantADP molecules per dimer are usually released during a single processive encounter with a MT. The results of Figure 7 indicate that the MT-stimulated rate of mantADP release for dimeric DKH405 is in fact faster with an ATP chase, $k_{bi-MT(T)}$, than with an ADP chase, $k_{bi-MT(D)}$. The MT-stimulated ADP release is highly sensitive to the concentrations of anions (*13*, *16*), and the observed bimolecular rate constant decreases significantly at higher ATP or ADP as indicated in Figure 7B,C. Extrapolation to zero nucleotide gives the true relative difference in rate for a chase with ATP versus ADP in the absence of an ionic contribution of the nucleotides. The ratio of $k_{bi-MT(D)}/k_{bi-MT(T)}$ is approximately 0.6 for dimeric DKH405, in agreement with a 1.67-pass process, which predicts a ratio of 0.6 (equal to 1/1.67). Note that the occupancy of the MT lattice by heads is low in this experiment, and thus ADP-induced dissociation must be fast even at low occupancy. With monomeric DKH357 (Figure 7C), the rate is independent of the chase nucleotide, as expected for initial mantADP release being a common rate-limiting step.

ATP-Stimulated Release of mantADP from the Tethered Intermediate. ATP induces the rapid release of ADP from the tethered intermediate, and this allows the dimer to remain attached to the MT as the tethered head becomes tightly bound on ADP release (*9*). A wide range of rates, however, have been reported for this reaction (*10*−*12*). A typical fluorescence transient for ATP stimulation of release of mantADP from the tethered intermediate of DKH405 at high ATP (2 mM) is indicated in the upper trace of Figure 8. The smooth line is the best fit for a single-exponential process over the range of 2.5−40 ms. The rate constant is 259 s^{-1}, but the fit shows systematic deviations. Inclusion of a linear steady-state term produces a fit that closely matches the observed transient and has a first-order rate constant of 326 s^{-1}. The average rates for eight transients were 325 ± 8 and 244 ± 4 s^{-1} for fits to a single exponential with and without a linear term, respectively. The lower trace in Figure 8 is the average of these eight transients. Analysis over a range of ATP concentrations yields a maximum rate of 360 s^{-1} and a $K_{0.5}$ value of 185 μM when fitted to an exponential with a linear term. Similar amplitudes for the transient were observed at all ADP and ATP concentrations with allowance for the loss expected for very fast reactions due to the ~1.7 ms dead time of the instrument. The calculated k_{bi-T} value of 2.0 μM^{-1} s^{-1} is in agreement with previous measurements (*10*, *12*).

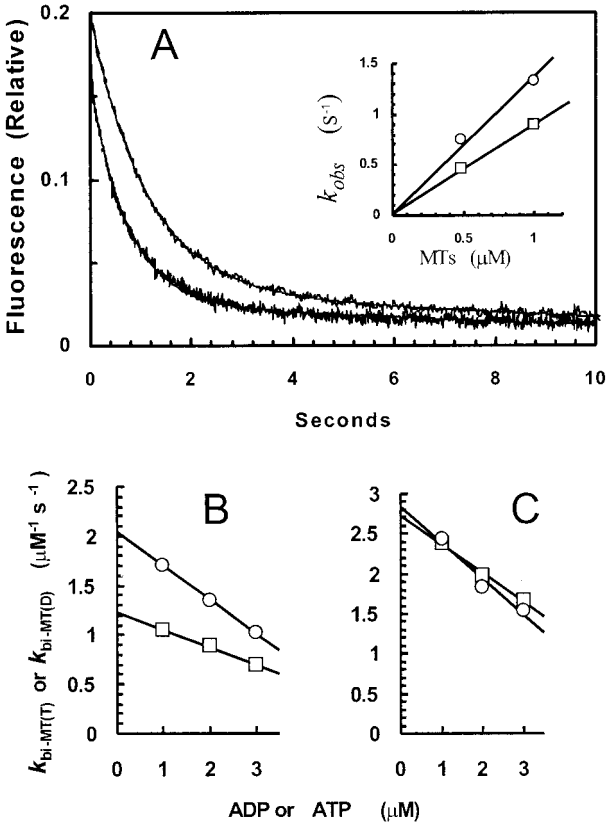

FIGURE 7: MT-stimulated mantADP release. The bimolecular rate for MT stimulation of mantADP release from DKH405·mantADP and DKH357·mantADP was determined in the presence of either excess ADP or ATP. One syringe contained 0.1 μM DKH405·mantADP or DKH357·mantADP with 0.25 μM extra mantADP (2× concentrations) to maintain saturation with mantADP, and the other syringe contained MTs with either MgADP or MgATP as indicated as final concentrations. The buffer was A25 supplemented with 50 or 25 mM KCl for DKH405 and DKH357, respectively. (A) Time course for DKH405 with 1 μM MTs and 2 mM ADP or ATP for the upper and lower trace, respectively. The thin line is the best fit for a first-order reaction with a linear steady-state component and gives rates of 0.89 and 1.34 s^{-1} for ADP and ATP, respectively. The insert is the dependence of the observed rate on the concentration of MTs: circles, MgATP; squares, MgADP. The k_{bi-MT} values obtained from the slopes are 0.89 and 1.32 μM^{-1} s^{-1}. (B and C) Secondary plots of the $k_{bi-MT(D)}$ and $k_{bi-MT(T)}$ values as a function of the ADP or ATP concentration for DKH405 (B) and DKH357 (C): circles, MgATP; squares, MgADP.

DISCUSSION

Release of ADP is the rate-limiting step in the absence of MTs, but binding to the MT induces rapid ADP release (*8*). The k'_o value for release of ADP from the tethered head in intermediate I at 0.05 s^{-1} is still slow but has been accelerated 5-fold compared to the rate of 0.01 s^{-1} for k_o in the absence of MTs (*5*). The extent to which the tethered head in II, III, or X interacts with the MT is not established, and this acceleration is potentially due to conformations in which the tethered head is bound to the MT. Drawing the tethered intermediates in Scheme 1 with the tethered head detached from the MT is not intended to indicate that this is the predominant conformation. It is also possible, however, that the acceleration is merely due to the highly charged ionic

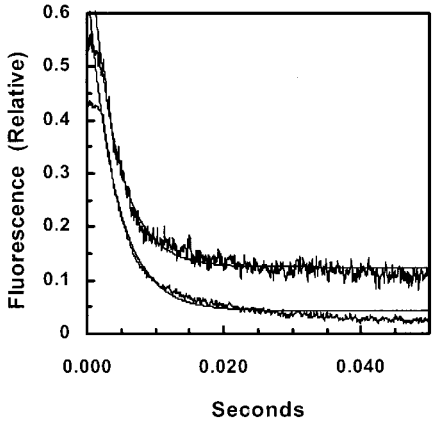

FIGURE 8: ATP-induced release of mantADP from the tethered intermediate. A stable DKH405·mantADP·MT tethered intermediate was generated from 6 μM MTs and 2 μM DKH405·mantADP and mixed 1:1 in the stopped flow with 4 mM MgATP (2×). The top trace is a single transient with the thin line being for a single-exponential process with a rate constant of 259 s^{-1} that was obtained from a fit to a first-order reaction over the time range of 2.5−40 ms. Note that the apparatus is designed to trigger data acquisition ~2 ms before flow stops so that the plateau level during flow can be observed. The lower trace is the average of eight individual traces, and the theoretical line is for a fit at 244 s^{-1}.

environment that the tethered head experiences on the surface of the MT (*17*) without any additional stereospecific interaction with the MT. The k_o value is known to be dependent on salt concentration, and the rate for basal release of mantADP from DKH365 increases 6-fold on increasing the KCl concentration from 25 to 800 mM [from 0.005 to 0.03 s^{-1} (*13*)].

Binding of ADP to the attached head of the tethered complex to produce intermediate III results in significant further acceleration of the release of the ADP from the tethered head. Although exact numerical assignment of rate constants is limited by the factors discussed below, the results of both turbidity and fluorescence experiments over a wide range of salt and MT concentrations are consistent with the model of Scheme 1, with rate constants of approximately 12 and 6 s^{-1} for $k_{off(D)}$ and $k_{t(D)}$, respectively. In this scheme, the fast phase of the biphasic fluorescence transient for mantADP release is due to direct ADP-stimulated release of mantADP via $k_{t(D)}$ that continues until terminated by dissociation via $k_{off(D)}$. The turbidity transient at 13 s^{-1} in 50 mM KCl directly monitors $k_{off(D)}$ for dissociation and agrees with the previous observation of Ma and Taylor (*16*). The fraction of the total mantADP that is released before initial dissociation will be determined by the partitioning of intermediate III and is equal to the ratio of $k_{t(D)}$ to the sum of $k_{t(D)}$ plus $k_{off(D)}$. The observed fractional amplitude of approximately one-third for the fast phase thus corresponds to a $k_{t(D)}$ value of 6 s^{-1} for a $k_{off(D)}$ of 12 s^{-1}. Interaction of the tethered head of III with the MT may be in part responsible for the reduced dissociation rate compared to monomers, but likely does not have a major energetic interaction with the MT because the dissociation rate of 12 s^{-1} is less than 5-fold reduced from the dissociation rate of monomeric DKH357 at 52 s^{-1} (*18*), as also discussed by Ma and Taylor (*10*). Furthermore, Thorn et al. (*19*) have shown that increasing the charge in the neck coil increases the processivity at zero load. Thus part of the reduction in the dissociation rate of DKH405 compared to monomers could be due to its highly charged coiled-coil region. Pechatnikova and Taylor (*20*) have reported evidence that the ADP-induced release of ADP from the tethered head of dimeric nonclaret disjunction protein (Ncd) also occurs by a two-pass process but without indication of partial release by a direct pathway.

Particularly, as analysis of the turbidity transient is complicated by its small amplitude and the flow artifact, it is important to note that this model is also supported by a number of other lines of evidence: (i) At high salt, the rate of dissociation is much faster than the slow phase, and further MT-stimulated release of mantADP must proceed through rebinding to the MT. (ii) The bimolecular rate for MT-stimulated mantADP release can be independently measured, and the rate for this bimolecular process is equal to the rate of the slow phase over a wide range of rates that are produced by different salt and MT concentrations. (iii) MTs added in trans are effective in accelerating the slow phase (trace c, Figure 5) as expected if they exert their influence bimolecularly. (iv) Bimolecular stimulation by MTs of mantADP release is faster when the chase nucleotide is ATP than when it is ADP, as expected if release in the presence of ADP is largely a double-pass process in which only 1.33 ADP molecules are released during each encounter of DKH405 with a MT.

This model predicts that the rate for the fast phase will be equal to the sum of $k_{off(D)}$ and $k_{t(D)}$. The small predicted decrease of only 33% between the rate for the fast phase of the fluorescence transient and the rate for the turbidity transient is likely within the considerable experimental uncertainties in evaluating the exact rate for the small turbidity change against a large mixing artifact and for extracting the rate of the fast phase from a fluorescence transient that is not cleanly biphasic. For example, the observed rate of 16.5 s^{-1} and fractional amplitude of 0.3 for the fast phase at 100 mM KCl (Figure 6) predict a rate of 11.6 s^{-1} for the turbidity transient that is probably not significantly different from the value of 15.3 s^{-1} observed in Figure 4.

The direct process for ADP-stimulated release of ADP from the tethered head does not necessarily require the type of directed conformational change proposed by Rice et al. (*21*) for the ATP-stimulated process. The weakly bound species of superfamily member Kif1A (*22*) can undergo lateral diffusion along the MT, and the attached head of III with bound ADP is analogous to these weakly bound species. Such increased flexibility in the attachment of III may allow the tethered head to release ADP in the absence of a specific directed conformation change. An additional complication is that intermediate II may have some fraction of its tethered head domains predocked in a position that is favorable for rapid release of ADP from the tethered head on nucleotide binding to the attached head. For example, the tethered head could be docked on the leading or trailing tubulin binding site. Thus the biphasic transients could also be due to two populations of II, which during initial ADP binding either preferentially releases ADP directly or preferentially dissociates from the MT.

Binding of ATP to the attached head produces a much larger acceleration of ADP release to ~300 s^{-1}. Detailed analysis is complicated by the deviations from a simple first-order reaction indicated in Figure 8. However, the bulk of

the transient (including the amplitude lost in the dead time) clearly occurs with a rate constant of ~300 s^{-1}, with the exact value depending on the particular model used to fit the data. Some of this complexity may result from a range of orientations and interactions of the tethered head prior to ATP binding as discussed above. Ma and Taylor (*10*) reported a lower value of 110 s^{-1}, but this result is not necessarily incompatible as their rate was determined at 20 °C with human kinesin rather than 25 °C with *Drosophila* kinesin and they fitted their transients to a simple exponential which yields a lower estimated rate as shown above. Johnson and co-workers (*23*) estimated $k_{t(T)}$ indirectly from reactions in which sequential release of both ADP molecules occurred following mixing of free kinesin with MTs. Their maximum extrapolated rate for this net reaction of 305 s^{-1} was originally interpreted in terms of a uniform site model that treated dimeric K401 as if it was a monomer. However, sequential release of both ADP molecules at equal rates requires that release of both the first ADP and the second ADP via $k_{t(T)}$ has values of 600 s^{-1} each. Subsequent reanalysis (*12*) indicated that the data were better accommodated by a maximum rate of 150 s^{-1} rather than 305 s^{-1}. This lowered value results in an estimated $k_{t(T)}$ value of 300 s^{-1} for equal rates at each step and is in good agreement with the direct measurement of $k_{t(T)}$ presented here. Other estimates have been considerably slower (*11*, *24*), and the cause of this difference is not obvious.

Implications for Processivity. Processivity can be limited by dissociation from all four principal intermediate states with bound ATP, ADP and P_i, ADP alone, or no nucleotide. This assumes that P_i release is faster than ADP release and an intermediate with bound P_i, but not bound ADP, does not accumulate. The tight binding in the absence of nucleotide and in the presence of AMP-PNP (*25*, *26*) suggests that dissociation of these complexes does not contribute significantly, although this has not been directly measured with ATP itself. With monomers, dissociation from the ADP state is likely to make a significant contribution (*18*, *27*). Monomeric MT·DKH357 is dissociated by ADP at 52 s^{-1} in 50 mM KCl (*18*), and a value of 65−90 s^{-1} was reported for human K332 (*27*). If the MT·DKH357·ADP intermediate generated during ATP hydrolysis releases ADP at 300 s^{-1}, then the fraction dissociating from the MT during each cycle will be given by $k_{off(D)}$ divided by the sum of $k_{off(D)}$ and k_D or 52 s^{-1}/(52 s^{-1} + 300 s^{-1}) = 0.142, which corresponds to an average of seven ATP molecules hydrolyzed before dissociation. This is in reasonable agreement with the observed $k_{bi-ratio}$ value of 4.4 for DKH357 in 120 mM potassium acetate (*5*), especially as some contribution to dissociation is also expected from the MT·DKH357·ADP·P_i intermediate. As discussed previously (*18*) the failure of monomers to dissociate during multiple ATP turnovers requires that dimers must accelerate the dissociation of the trailing head following hydrolysis in order to ensure that dissociation occurs during each ATPase cycle at 80 s^{-1} per dimer. Single-headed dimers are reported to have a much lower net dissociation rate (*28*). More extensive processivity can also occur with monomer in some cases as discussed below.

For dimers, a strictly sequential pathway for hydrolysis that proceeds from II to IV, V, VII, and back to II (Scheme 2) would approach infinite processivity because one head or the other is always tightly bound in either the ATP or nucleotide-free state. There is, however, no evidence that requires that ATP-induced ADP release and hydrolysis are strictly sequential. The MT complex of monomeric DKH357 hydrolyzes ATP at an initial rate of 100 s^{-1} (*18*), and this may be a good model of hydrolysis in IV with only one head strongly attached to the MT. The net rate for hydrolysis and P_i release cannot be much slower than 100 s^{-1} because a value of 300 s^{-1} for $k_{t(T)}$ and a steady-state rate of 80 s^{-1} per dimer leaves only 110 s^{-1} total rate limitation in the rest of the cycle for a scheme that is mainly sequential. The hydrolysis of species IV to yield species VI and III thus provides an attractive possible route for dissociation from the MT. Most of species VI may rapidly release P_i and most of species III will revert to species II by ADP release from the attached head at ~300 s^{-1}, but species III can also yield species II′ via $k_{t(D)}$ at 6 s^{-1} or dissociate from the MT via $k_{off(D)}$ at 12 s^{-1}. The fraction of ATPase cycles that result in dissociation from III will be given by the fraction of IV that partitions to III times the fraction of III that partitions to I. Using k_{hyd} at 100 s^{-1} as an approximation of the rate for conversion of IV to III, this fraction is $[k_{hyd}/(k_{hyd} + k_{t(T)})][k_{off(D)}/(k_{off(D)} + k_{t(D)} + k_D)] = 0.25 \times 0.038 = 0.0094$ and corresponds to an average of 1/0.0094 = 106 ATP molecules hydrolyzed before dissociation. Some additional dissociation is also possible from VI. This predicted extent of processivity is essentially identical to the estimate based on the $2k_{bi-ratio}$ value of ~100 ATP molecules hydrolyzed per dimer before dissociation.

In effect, the hydrolysis reaction appears to be acting like a clock that starts ticking when ATP binds to the attached head of the tethered intermediate. If intermediate IV does not rapidly get the tethered head into the tight binding mode through release of ADP via $k_{t(T)}$, then hydrolysis will occur with formation of species with increased potential for dissociation from the MT. Although the fraction that dissociates could be reduced by decreasing the hydrolysis rate, this would also directly reduce the sliding velocity. Alternatively, the extent of processivity could be increased by increasing the value of $k_{t(T)}$, but this process is already fast,

Scheme 2: Scheme for Processive ATP Hydrolysis[a]

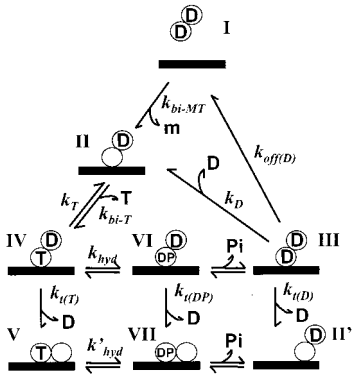

[a] Generally after Scheme 1 with the same numbering for intermediates and with ATP represented by T and phosphate by P or P_i. Note that no directed movement of the attachment point of the tethered dimer on the MT is intended on going from III to II′ via the tethered transition with ADP, $k_{T(D)}$, as discussed in the legend to Scheme 1. The indicated movement is for the ATP-dependent process from IV to II′ via $k_{T(T)}$. ATP can likely bind to VII as discussed in the Discussion, but this pathway is not indicated for clarity.

and a significant further increase in rate may not be readily possible. A decrease in the rate of release of III from the MT would also increase the extent of processivity, and this is likely a factor in the increased processivity observed with an increase in charge in the neck coil (*19*) or in loop 12 (*29*, *30*). An additional feature of this analysis is that one-fourth of the ATP is wasted in a futile cycle as most of the species III that is formed reverts to species II without generation of movement. Similarly, direct release of P_i from VII would also result in a bound head with ADP and lead to rapid unproductive ADP release. During processive cycling, dissociation of the trailing head with ADP and P_i still bound could potentially circumvent futile cycling by this pathway. The possibility of such futile cycles has also been considered by Crevel et al. (*24*).

Scheme 2 is a highly simplified model that can be expanded as additional information becomes available. Because P_i release is likely to be fast, it is not currently possible to estimate the amount of dissociation that occurs from VI or the rate that VI converts to VII. The observed rate of $\sim$300 s^{-1} for ATP-induced ADP release from II will have contributions from both $k_{t(T)}$ and $k_{t(DP)}$ because 300 s^{-1} is not much faster than hydrolysis. It is also not known if the intermediate II′ that forms transiently during steady-state hydrolysis has the same properties as the stable intermediate II formed by mixing kinesin with MTs. Additionally, ATP binding to the empty head of VII could directly generate IV and bypass formation of II′ altogether. This would allow part of the energy of ATP binding to be used to accelerate dissociation of the trailing head in VII, but might also significantly reduce the effective rate of ATP-stimulated ADP release because ATP binding to VII must first effect dissociation and P_i release to form IV before it can stimulate ADP release to form V. It will be of interest to determine the cause of the altered processivity observed in constructs with altered neck regions (*19*, *31*).

Analysis of dimeric DKH405 as presented here indicates that it is highly processive with 50−60 ATP molecules hydrolyzed per head per productive encounter with a MT, whereas Johnson and co-workers (*12*, *23*, *32*) have concluded that dimers are only marginally processive. The average number of ATP molecules hydrolyzed per productive encounter with a MT is equal to the ratio of the bimolecular rates for MT-stimulated ATPase relative to initial ADP release (*4*, *5*). For dimeric K401 at moderate salt concentration this ratio was reported to be 1 (*23*), which indicates a completely nonprocessive motor. Limited processivity was observed at low salt, and a revised analysis concluded that just 3−5 ATP molecules are hydrolyzed per head per encounter over a range of salt concentrations (*12*). These low values reported for K401 are incompatible with the motile properties of kinesin, which indicate that $\sim$80 ATP molecules are hydrolyzed per head per encounter (*31*). These low estimates of the processivity of K401 are largely due to the use of 13.6 s^{-1} for the net rate of dissociation of K401 from the MT during ATP hydrolysis (*23*). Dimeric kinesin exhibits overcrowding artifacts when the MT lattice is partially saturated with bound motors (*33*), and the rate of dissociation for K401 was obtained under conditions where accelerated dissociation due to overcrowding would be expected. The rate of dissociation from the MT during steady-state ATP hydrolysis under conditions of low lattice occupancy for DKH405 has not been determined directly but can be calculated from $(K_{0.5MT})(k_{bi-ADP}) = 0.143\ \mu M \times 5.7\ \mu M^{-1}\ s^{-1} = 0.8\ s^{-1}$. The analyses also differ in the step that is responsible for net dissociation of the dimer that terminates a processive run during ATP hydrolysis. The rate $k_{off(D)}$ value for dissociation of species II is zero in the analysis of Gilbert et al. (*12*), whereas dissociation of this intermediate is measured here at $\sim$12 s^{-1}.

Moyer et al. (*32*) also concluded that kinesin monomers were much more processive than dimers on the basis of kinetic processivity values of 18 for monomeric K341 and 3−5 for dimers. Our previous analysis (*5*) reached the opposite conclusion that monomers were much less processive than dimers with corresponding values of $\sim$4 and $\sim$50 for monomer and dimers, and this conclusion is further supported by the work presented here. This discrepancy is due both to the underestimate of the processivity of dimers by Moyer et al. (*32*), as discussed above, and to their use of K341 as a model for a monomer head domain for comparison to dimers. Although the comparable DKH340 was originally used as a model monomer (*14*, *34*), a subsequent study of an extensive series of truncations in the neck region (*5*) established that the properties of DKH340 were significantly different from those of longer monomers. While DKH346, DKH357, and DKH365 are all only moderately processive with $\sim$4 ATP molecules hydrolyzed before dissociation, DKH340 has a decreased rate of dissociation that results in hydrolysis of 28 ATP molecules before dissociation (*5*). Thus the inclusion of just a few additional amino acids to produce DKH346 with a complete neck linker results in a radical change from the properties of DKH340 or K341 with a truncated neck linker. A structural basis for the altered properties of short monomers was provided by the later solution of the crystal structure of a long rat kinesin monomer with the neck linker in the docked position (*35*). In this structure the region homologous to *Drosophila* 342−344, which is deleted in short monomers, makes significant contacts with the core motor domain. The contacts between these regions in the structure of dimeric rat kinesin (*36*) are less extensive, but there is still a hydrogen bond between the amide nitrogen of E342 (*Drosophila* numbering) and a backbone carbonyl group in the core domain that contributes to the docking interaction. Truncation to position 340 or 341 would result in disruption of these interactions between the neck linker and the core motor domain and will likely result in significant changes in ΔG for the docking reaction and the rate constants for steps in coupled ATP hydrolysis and MT interaction. It is of interest to determine the mechanistic basis for the reduced dissociation rate of constructs truncated in the neck linker region such as DKH340 and K341, especially as it may relate to the very low dissociation rates observed with other superfamily members such as Kif1A (*22*) and some kinesin constructs (*37*). However, these short constructs may be poor models for the properties of a single full-length head in a native dimer.

ACKNOWLEDGMENT

I thank Jing-Qui Cheng for construction of the housing for the stirred fluorescence observation cell, Maryanne Stock for preparation of DKH405, and the Drug Synthesis and Chemistry Branch of the National Cancer Institute for Taxol.

REFERENCES

1. Hirokawa, N., Noda, Y., and Okada, Y. (1998) *Curr. Opin. Cell Biol. 10*, 60−73.
2. Howard, J., Hudspeth, A. J., and Vale, R. D. (1989) *Nature 342*, 154−158.
3. Svoboda, K., Schmidt, C. F., Schnapp, B. J., and Block, S. M. (1993) *Nature 365*, 721−727.
4. Hackney, D. D. (1995) *Nature 377*, 448−450.
5. Jiang, W., Stock, M., Li, X., and Hackney, D. D. (1997) *J. Biol. Chem. 272*, 7626−7632.
6. Hancock, W. O., and Howard, J. (1998) *J. Cell Biol. 140*, 1395−1405.
7. Coy, D. L., Wagenbach, M., and Howard, J. (1999) *J. Biol. Chem. 274*, 3667−3671.
8. Hackney, D. D. (1988) *Proc. Natl. Acad. Sci. U.S.A. 85*, 6314−6318.
9. Hackney, D. D. (1994) *Proc. Natl. Acad. Sci. U.S.A. 91*, 6865−6869.
10. Ma, Y. Z., and Taylor, E. W. (1997) *J. Biol. Chem. 272*, 724−730.
11. Lockhart, A., Cross, R. A., and McKilop, D. F. A. (1995) *FEBS Lett. 368*, 531−535.
12. Gilbert, S. P., Moyer, M. L., and Johnson, K. A. (1998) *Biochemistry 37*, 792−799.
13. Cheng, J. Q., Jiang, W., and Hackney, D. D. (1998) *Biochemistry 37*, 5288−5295.
14. Huang, T.-G., and Hackney, D. D. (1994) *J. Biol. Chem. 269*, 16493−16501.
15. Williams, R. C., Jr., and Lee, J. C. (1982) *Methods Enzymol. 85*, 376−385.
16. Ma, Y. Z., and Taylor, E. W. (1995) *Biochemistry 34*, 13242−13251.
17. Baker, N. A., Sept, D., Joseph, S., Holst, M. J., and McCammon, J. A. (2001) *Proc. Natl. Acad. Sci. U.S.A. 98*, 10037−10041.
18. Jiang, W., and Hackney, D. D. (1997) *J. Biol. Chem. 272*, 5616−5621.
19. Thorn, K. S., Ubersax, J. A., and Vale, R. D. (2000) *J. Cell Biol. 151*, 1093−1100.
20. Pechatnikova, E., and Taylor, E. W. (1999) *Biophys. J. 77*, 1003−1016.
21. Rice, S., Lin, A. W., Safer, D., Hart, C. L., Naber, N., Carragher, B. O., Cain, S. M., Pechatnikova, E., Wilson-Kubalek, E. M., Whittaker, M., Pate, E., Cooke, R., Taylor, E. W., Milligan, R. A., and Vale, R. D. (1999) *Nature 402*, 778−784.
22. Okada, Y., and Hirokawa, N. (1999) *Science 283*, 1152−1157.
23. Gilbert, S. P., Webb, M. R., Brune, M., and Johnson, K. A. (1995) *Nature 373*, 671−676.
24. Crevel, I., Carter, N., Schliwa, M., and Cross, R. (1999) *EMBO J. 18*, 5863−5872.
25. Lasek, R. J., and Brady, S. T. (1985) *Nature 316*, 645−647.
26. Vale, R. D., Reese, T. S., and Sheetz, M. P. (1985) *Cell 42*, 39−50.
27. Ma, Y. Z., and Taylor, E. W. (1997) *J. Biol. Chem. 272*, 717−723.
28. Hancock, W. O., and Howard, J. (1998) *J. Cell Biol. 140*, 1395−1405.
29. Okada, Y., and Hirokawa, N. (2000) *Proc. Natl. Acad. Sci. U.S.A. 97*, 640−645.
30. Rogers, K. R., Weiss, S., Crevel, I., Brophy, P. J., Geeves, M., and Cross, R. (2001) *EMBO J. 20*, 5101−5113.
31. Romberg, L., Pierce, D. W., and Vale, R. D. (1998) *J. Cell Biol. 140*, 1407−1416.
32. Moyer, M. L., Gilbert, S. P., and Johnson, K. A. (1998) *Biochemistry 37*, 800−813.
33. Hackney, D. D. (1994) *J. Biol. Chem. 269*, 16508−16511.
34. Huang, T.-G., Suhan, J., and Hackney, D. D. (1994) *J. Biol. Chem. 269*, 16502−16507.
35. Sack, S., Muller, J., Marx, A., Thormahlen, M., Mandelkow, E. M., Brady, S. T., and Mandelkow, E. (1997) *Biochemistry 36*, 16155−16165.
36. Kozielski, F., Schonbrunn, E., Sack, S., Muller, J., Brady, S. T., and Mandelkow, E. (1997) *J. Struct. Biol. 119*, 28−34.
37. Inoue, Y., Iwane, A. H., Miyai, T., Muto, E., and Yanagida, T. (2001) *Biophys. J. 81*, 2838−2850.

BI0159229